Martensitic transformation, twin boundary and phase interface mobility of directionally solidified Ni-Mn-Ga alloys during compression by EBSD tracing

Yanchao Dai[1], Long Hou[1], Yves Fautrelle[2], Zongbin Li[3], Claude Esling[4], Zhongming Ren[1], Xi Li [1,2,*]

[1]State Key Laboratory of Advanced Special Steels, Shanghai University, Shanghai, 200072, P. R. China
[2]EPM-Madylam, ENSHMG BP 38402 St Martin d'HeresCedex, France
[3]Key Laboratory for Anisotropy and Texture of Materials, Northeastern University, Shenyang 110819, P. R. China
[4]Laboratoire d'Étude des Microstructures et de Mécanique des Matériaux (LEM3), CNRS UMR 7239, Université de Lorraine, 57045 Metz, France

Abstract. Directionally solidified Ni-Mn-Ga alloy with orderly arrayed austenite and non-modulated martensite (NM) was formed due to microsegregation between dendrite arm and interdendritic region, leading to preferred orientation of $<001>_A$ and $<110>_M$ coexistence at ambient temperature. The stress-induced martensitic transformation took place due to the increase of martensitic transformation temperature under step-wise uniaxial compression. The detwinning process accompanied with dislocation mobility was easy to carry out on the twin planes 45° inclined to the compression axis, compared with the twin planes parallel to the compression axis in the dominant twinned groups. The martensitic transformation and reorientation of variants were investigated by electron backscatter diffraction.

1. Introduction

Ni-Mn-Ga ferromagnetic shape memory alloys (FSMAs) with giant magnetic field-induced strains (MFIS) in the martensitic phase have been widely investigated as a kind of promising materials for actuator and sensor [1-4]. A 12% MFIS in non-modulated (NM) tetragonal crystal structure has been achieved by modifying the Ni-Mn-Ga alloy's composition with Co and Cu additives, which considerably decrease the twinning stress of the alloy [5]. Therefore, the key requirements to obtain considerable MFIS are high magnetocrystalline anisotropy and low twinning stress [3, 6]. It is relatively

easy to obtain Ni-Mn-Ga single crystals with microstructure of multiple martensite variants, provided that they are subjected to a necessary training process [7]. The uniaxial compression tests are usually applied along $<001>_A$ directions referred to high temperature austenite phase. As the shape change is anisotropic, imposition of a unidirectional constraint (tension or compression) can promote the formation of some favorable variants [8]. Therefore, the application of an external load during the martensitic transformation is an effective method to modify the variant distribution [9, 10].

The characteristics of the final martensite phase are closely related to the crystallographic orientation and microstructure of the parent austenite [11]. An austenite with preferred orientation is generally easy to obtain by directional solidification (DS) [12-14]. Moreover, the samples prepared by DS with high growth speed will produce microsegregation based on our previous research [15]. Considering that the transformation temperature is sensitive to the composition in Ni-Mn-Ga alloys, the characteristic in DS can be used to prepare multi-phase mixed microstructures. In this paper, orderly arrayed two-phase Ni-Mn-Ga alloy prepared by DS makes it possible that the coupling of stress-induced martensitic transformation and variant reorientation can be shown and analyzed in detail at ambient temperature. It simplifies the measured difficulty of in-situ observation because there is no thermally-induced process. The electron backscatter diffraction (EBSD) measurement used in this work is highly visualized and suitable for observing the stress-induced processes at different stages. The martensitic transformation processes under step-wise uniaxial compression were traced and direct evidence of the detwinning process induced by stress was captured.

2. Experimental details

The alloy with nominal composition $Ni_{46.7}Mn_{33.9}Ga_{19.4}$ (at.%) was prepared in an arc-melting furnace under an argon atmosphere from high-purity Ni (99.99 wt.%), Mn (99.9 wt.%) and Ga (99.99 wt.%). 2 wt.% excess Mn was added in order to compensate for the Mn loss during melting. The ingots were remelted five times for homogeneity. The experimental apparatus consisted of a Bridgman-Stockbarger-type furnace equipped with a pulling system and a temperature controller. The furnace was heated to 1450°C and held for an hour. Then the specimen was directionally solidified in the Bridgman apparatus by drawing the crucible assembly at a constant speed of 20 μm/s into the liquid Ga-In-Sn metal (LMC) cylinder. A sample with ϕ 3 mm × 6 mm was cut from a stable growth zone in the directionally solidified rod. The compression process was performed with a MTS809 material testing system. Uniaxial compression tests were conducted along the direction of DS with a constant speed of 0.15 mm/min at room temperature.

The compositional variation of the ternary alloy was measured by energy dispersive spectroscopy (EDS) (Octane Plus, EDAX), working at 25 kV. The crystal orientations of austenite and martensite at ambient temperature were characterized in a Hitachi SU70 scanning electron microscope with EBSD acquisition camera and OIM software provided by EDAX Instruments. The identical cross section was measured by EBSD before and after each compression step. The sample after each compression step needed a repolish in order to obtain a high indexing rate. The loss as little as possible was accomplished when using 3000 grit sandpaper. After that the sample was prepared using electropolished (Lectropol-5, Struers™) with a solution of nitric acid (20 vol.%) and methanol (80 vol.%). The EBSD scanning was carried out at 25 kV, over 1/4 cross section and the detailed maps were detected with a step size of 2 μm and 0.5 μm. The raw data obtained in this study were processed using OIM software. Grain confidence

index (CI) standardization and Grain dilation were selected to clear up the noise. The data with high CI value (CI > 0.3) were selected.

3. Results and discussion

Fig. 1 shows the distribution of austenite and martensite variants at the steady solid phase zone of directionally solidified Ni-Mn-Ga alloy rod. It is worth noting that the orientations of non-modulated martensite are all indexed according to the tetragonal $L1_0$ unit cell [16, 17]. Considering that the lattice parameter of the two phases in directionally solidified alloys varies due to the microsegregation, the Bain model is used to give a simplified but competent description of the variant distribution. The transformation from cubic parent phase to tetragonal martensitic phase based on the Bain relationship would result in three different martensite variants [18]. The c-axis of each variant is parallel to one principle axis of the cubic parent phase. The representative relationship is $(001)_A//(001)_M$ and $[100]_A//[1\text{-}10]_M$. Fig. 1(a) shows the IPF map of the cross section at the steady solid phase zone. The

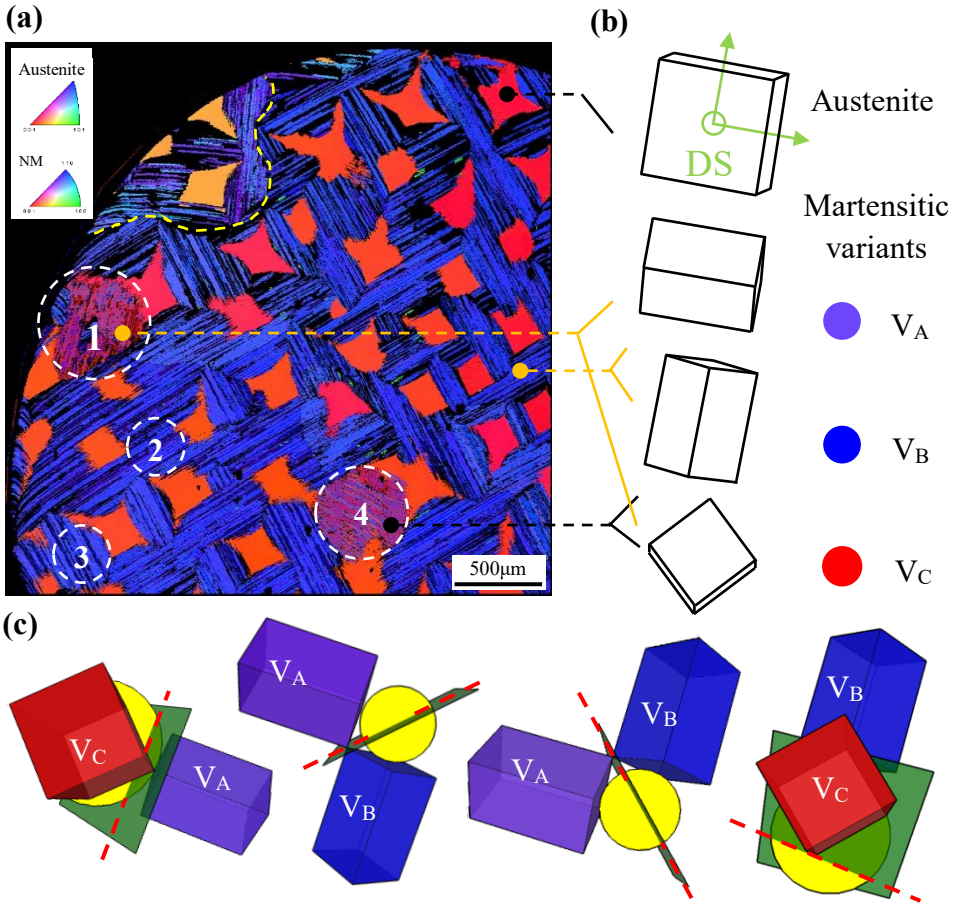

Figure 1. The distribution of austenite and martensite variants at the steady solid phase zone of directionally solidified Ni-Mn-Ga alloy rod. (a) IPF map of the cross section; (b) Orientations of unit cell for twin variants. (c) Geometric perspective views corresponding to the twin orientation relationships of the four variant groups. The unit cell orientations agree with the real ones from the EBSD data. Intersection lines (red) between the twin planes (green) and the sample surface planes (yellow) correspond to the IPBs within the white dotted circles of the EBSD map.

austenite shaped like a star or square is uniformly distributed in the martensitic matrix. The orientation of the residual austenite was verified as $<001>_A$ preferred orientation along the solidification direction for the whole grain before martensitic transformation. The martensite phase has a $<110>_M$ preferred orientation in the cross section. Orientations of the unit cell for twin variants are displayed in Fig. 1(b). It shows that all three variants are all generated in the cross section and each pair of variants creates a colony separated by an intercolony boundary (ICB) [19]. Four representative regions are selected from the colonies and marked with white circles. Within each colony, martensite variants are separated by an interplate boundary (IPB) [19]. The twin orientation relationships for the four variant groups are illustrated by geometric perspective views, which contain three oriented variants named V_A, V_B and V_C (see Fig. 1(c)). Variant groups 2 and 3 both composed of V_A and V_B take up the major parts of the martensite phase. The IPBs in the two main colonies are crisscross and orthogonal. The IPBs in variant groups 1 and 4 are inclined at about ~45° regarding the ones in variant groups 2 and 3. Variant group 1 (consisting of V_A and V_C) and variant group 4 (consisting of V_B and V_C) are not the main twinned structures in the preferential oriented DS rod. It should be pointed out that different martensite variants arrange themselves into variant groups in order to minimize the internal stress [20]. All transformations, free from external stress, tend to be self-accommodating since the shape change in any group will produce a stress field favoring the formation of some particular variants [21].

The mixed austenitic-martensitic zone is derived from the microsegregation between dendrite core and interdendritic region. The microstructure of the longitudinal section of directionally solidified Ni-Mn-Ga alloy is shown in Fig. 2. The strip-shaped areas at the stable solid phase zone represent

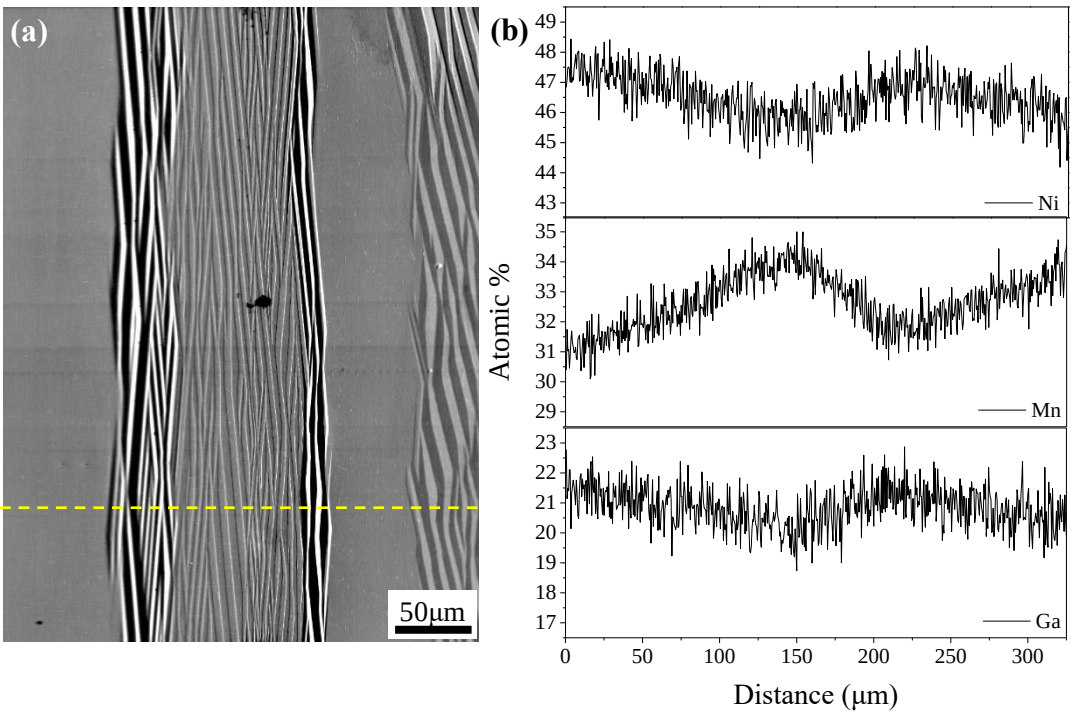

Figure 2. (a) SEM micrograph of the mixed austenitic-martensitic zone in longitudinal section. (b) Distribution of three elements the dashed line measured by EDS.

martensite and the surrounded parts signify austenite. They are also corresponding to the interdendritic region and dendrite core. The distribution of three elements along the dashed line is displayed in Fig. 2(b). It is found that the fluctuation of Mn is more obvious than that of Ni and Ga. The Ni-rich, Mn-poor and Ga-rich composition corresponds to the dendrite core region, while Ni-poor, Mn-rich and Ga-poor composition is found in the interdendritic region. The composition variation results in a change of the e/a value. Generally speaking, the martensitic transformation temperature is linearly depending on e/a values [22]. The martensite embryos initially form near the e/a peak with a high martensitic transformation temperature. As a result, they are constrained by the surrounding austenite with a lower valence electron concentration in the dendrite core and show a preferential variant distribution due to the constraints by their surrounding with lower e/a value.

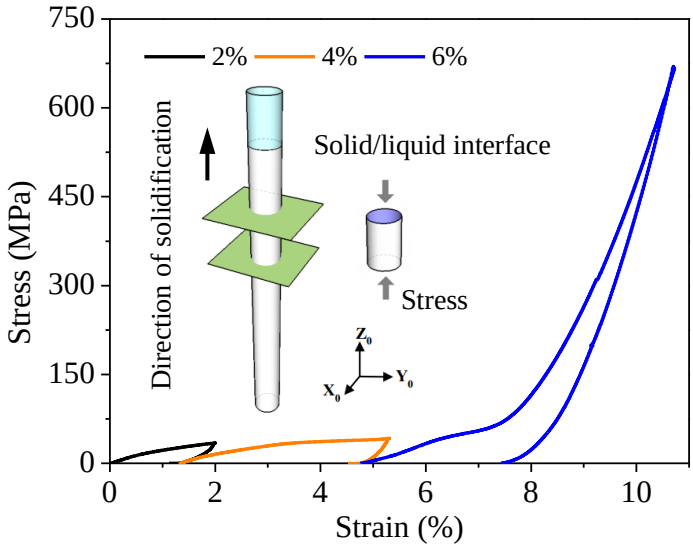

Figure 3. The stress-strain curves obtained from step-wise compression and unloading experiments along the direction of directional solidification.

Fig. 3 shows the stress-strain curves obtained from step-wise uniaxial compression loading and unloading. The hierarchic stress-strain curves manifest the step-wise compressive deformations to strains of 2%, 4% and 6%. The strains are all based on the original length of the column. A conspicuous stress plateau means the twin boundaries become mobile and the reorientation process of the variants starts. The microstructural changes in the directionally solidified two-phase Ni-Mn-Ga alloy subjected to interrupted straining tests were monitored by EBSD, as shown in Fig. 4. It should be noted that the EBSD data were taken from the identical cross section after each cycle of loading and unloading. It is found that the volume fraction of austenite begins to reduce when the strain increased from 2% to 4% and utterly disappears at a strain of 6%.

The detailed transformations of twin boundary and phase interface mobility are depicted in Fig. 4. IPF maps are displayed in the same area before compression and after 4% and 6% strain. The twin and phase boundaries moved at the same time under the uniaxial compression. The reorientation of

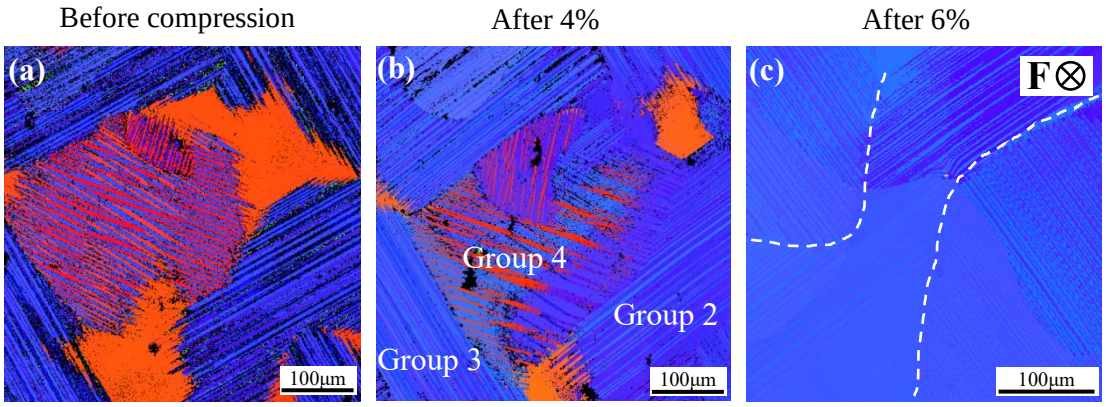

Figure 4. EBSD IPF maps of a magnified region in Ni-Mn-Ga alloy during step-wise compression: (a) before compression; (b) after 4%; (c) after 6%. F means the direction of applied stress. The white dashed lines represent the ICBs between residual group 2 and 3.

martensite variants was accompanied by detwinning. The twin boundaries in group 4 of Fig. 4(b) are curved and irregular. The movement of the twin boundaries in this area can be observed after the first two cycles (2% and 4% strain). In addition, a small dominance of V_B in group 4 (blue color in the middle area) can be noticed. The non-uniform distribution of martensite variants during mechanical training has also been justified [23, 24]. The twin plane in group 4 is at ~45° with respect to the compression axis. The corresponding Schmid factor is close to 0.5. However, V_A and V_B in surrounding of group 2 and 3 keep an uniform distribution after three cycles uniaxial compression along $[001]_A$. As the twin plane is aligned almost parallel to the compression axis, the Schmid factor for any detwinning system potentially operating within this plane is close to zero. The critical detwinning stress cannot be reached to reorient one variant to the other and drive twin boundary motion. After the third cycle in Fig. 4(c), the austenite and variant V_C disappear completely. The group 4 is consumed by the combination of V_A and V_B and the IPBs in adjacent colonies are orthogonal to each other.

4. Conclusions

The influence of step-wise uniaxial compression on the martensitic transformation and detwinning process was investigated in a directionally solidified Ni-Mn-Ga alloy by EBSD. Because of composition segregation, the martensitic transformation temperature gradually increases from the core to the edge of the dendrite, leading to the coexistence of martensite and austenite at ambient temperature. The alloy undergoes a coupling of martensitic transformation and variant reorientation under uniaxial compression. The martensite groups composed of V_C and V_A or V_B with twinning planes inclined to the compression axis at ~45° are detwinned under uniaxial compression, which agrees with the calculated Schmid factor (~0.5).

Acknowledgements

We are grateful to the demo Lab of EDAX China providing the support for EBSD measurement. The authors would like to thank for the financial support from National foundation of Science (Nos. 51690164, 51571056, 51431005), “Shuguang Program” from Shanghai Municipal Education

Commission and the Program for Professor of Special Appointment (Eastern Scholar) at Shanghai Institutions of Higher Learning and Science and Technology Commission of Shanghai Municipality (No. 11JC1413600) and Shanghai Science and Technology Committee Grant (13DZ1108200, 13521101102) and United Innovation Program of Shanghai Commercial Aircraft Engine (AR910, AR911).

[1] Ullakko K, Huang J, Kantner C, OHandley R, Kokorin V. Large magnetic - field - induced strains in Ni2MnGa single crystals. Applied Physics Letters 1996;69:1966-8.
[2] O'Handley RC. Model for strain and magnetization in magnetic shape-memory alloys. Journal of Applied Physics 1998;83:3263.
[3] Sozinov A, Likhachev A, Lanska N, Ullakko K. Giant magnetic-field-induced strain in NiMnGa seven-layered martensitic phase. Applied Physics Letters 2002;80:1746.
[4] Chernenko VA, Anton RL, Kohl M, Barandiaran JM, Ohtsuka M, Orue I, et al. Structural and magnetic characterization of martensitic Ni–Mn–Ga thin films deposited on Mo foil. Acta Materialia 2006;54:5461-7.
[5] Sozinov A, Lanska N, Soroka A, Zou W. 12% magnetic field-induced strain in Ni-Mn-Ga-based non-modulated martensite. Applied Physics Letters 2013;102:021902.
[6] James RD, Tickle R, Wuttig M. Large field-induced strains in ferromagnetic shape memory materials. Materials Science and Engineering: A 1999;273–275:320-5.
[7] Sozinov A, Likhachev AA, Lanska N, Soderberg O, Ullakko K, Lindroos VK. Stress- and magnetic-field-induced variant rearrangement in Ni-Mn-Ga single crystals with seven-layered martensitic structure. Materials Science and Engineering a-Structural Materials Properties Microstructure and Processing 2004;378:399-402.
[8] Wang YD, Brown DW, Choo H, Liaw PK, Cong DY, Benson ML, et al. Experimental evidence of stress-field-induced selection of variants in Ni-Mn-Ga ferromagnetic shape-memory alloys. Physical Review B 2007;75.
[9] Li ZB, Zhang YD, Esling C, Gan WM, Zou NF, Zhao X, et al. In-situ neutron diffraction study of martensitic variant redistribution in polycrystalline Ni-Mn-Ga alloy under cyclic thermo-mechanical treatment. Applied Physics Letters 2014;105.
[10] Li Z, Zou N, Yang B, Gan W, Hou L, Li X, et al. Effect of compressive load on the martensitic transformation from austenite to 5M martensite in a polycrystalline Ni–Mn-Ga alloy studied by in-situ neutron diffraction. Journal of Alloys and Compounds 2016;666:1-9.
[11] Liu J, Zheng H, Huang Y, Xia M, Li J. Microstructure and magnetic field induced strain of directionally solidified ferromagnetic shape memory CoNiAl alloys. Scripta Materialia 2005;53:29-33.
[12] Jiang C, Liu J, Wang J, Xu L, Xu H. Solid–liquid interface morphology and crystal growth of NiMnGa magnetic shape memory alloys. Acta Materialia 2005;53:1111-20.
[13] Liu J, Zheng HX, Li JG. Effect of solidification rate on microstructure and crystal orientation of ferromagnetic shape memory alloys Co–Ni–Al. Materials Science and Engineering: A 2006;438-440:1061-4.
[14] Wang J, Jiang C. Single-crystal growth of NiMnGa magnetic shape memory alloys. Journal of Crystal Growth 2008;310:865-9.
[15] Li X, Gagnoud A, Ren Z, Fautrelle Y, Debray F. Effect of strong magnetic field on solid solubility and microsegregation during directional solidification of Al-Cu alloy. Journal of Materials Research 2013;28:2810-8.
[16] Niemann R, Fähler S. Geometry of adaptive martensite in Ni-Mn-based Heusler alloys. Journal of Alloys and Compounds 2017;703:280-8.
[17] Pons J, Chernenko VA, Santamarta R, Cesari E. Crystal structure of martensitic phases in Ni–Mn–Ga shape

memory alloys. Acta Materialia 2000;48:3027-38.
[18] Bain EC. Nature of martensite. Trans AIME 1924;70:25–46.
[19] Szczerba MJ, Chulist R. Detwinning of a non-modulated Ni–Mn–Ga martensite: From self-accommodated microstructure to single crystal. Acta Materialia 2015;85:67-73.
[20] Christian JW. Deformation by moving interfaces. Metallurgical Transactions A 1982;13:509-38.
[21] Zhu JJ, Huang WM, Liew KM. Deformation energy in martensitic transformation. J Phys IV 2003;112:179-82.
[22] Chulist R, Sozinov A, Straka L, Lanska N, Soroka A, Lippmann T, et al. Diffraction study of bending-induced polysynthetic twins in 10M modulated Ni-Mn-Ga martensite. Journal of Applied Physics 2012;112:063517.
[23] Zhou L, Giri A, Cho K, Heinrich H, Majumdar BS, Sohn Y. Microstructural and Crystallographic Characterization of Ni2+x Mn1−x Ga Alloys (x = 0.14, 0.16, 0.19, 0.22, and 0.24) by Transmission Electron Microscopy. Metallurgical and Materials Transactions E 2014;1:239-46.
[24] Szczerba MJ, Chulist R, Kopacz S, Szczerba MS. Effect of initial plastic strain on mechanical training of non-modulated Ni–Mn–Ga martensite structure. Materials Science and Engineering: A 2014;611:313-9.